Transition Metal Chemistry (2024) 49:67–74
https://doi.org/10.1007/s11243-023-00562-7

A novel Cd(II) compound of flucytosine: synthesis, structure, and optical properties

Hela Ferjani[1] · N. S. Almotlaq[1] · Mohammed Fettouhi[2,3] · Murendeni P. Ravele[4,5] · Damian C. Onwudiwe[4,5]

Received: 8 August 2023 / Accepted: 16 October 2023 / Published online: 3 November 2023

Abstract

Background The study and development of fluorouracil metal complexes are important in the development of new synthetic methods and materials with applications in pharmaceuticals, agrochemicals, and materials science.

Mothodology A new Cd(II) compound, (H-5FC) [(H-5FC) Cd Cl] (1), (where H-5FC is HFlucytosine), was successfully synthesized and crystallized by slow evaporation at room temperature. The compound was characterized by single-crystal X-ray diffraction technique and UV–Visible spectroscopy.

Results The structure shows that the compound constitutes of an independent protonated $(H\text{-}5FC)^{+}$ cation and two protonated flucytosine molecules that coordinate to the Cd(II) ion via an oxygen atom to form a trinuclear $[(H\text{-}5FC)_2Cd_3Cl_{10}]^{2-}$ anionic moieties. The independent protonated $(H\text{-}5FC)^{+}$ bridges the $[(H\text{-}5FC)_2Cd_3Cl_{10}]^{2-}$ anions via N/C–H···Cl/O hydrogen bonds. Supramolecular structure analysis of (1) with the aid of Hirshfeld calculations showed the importance of the H···Cl, O···H, C···Cl, and F···Cl interactions. Their percentages were calculated to be 42.2, 10.3, 6.6, and 8.7%, respectively. The band gap energy of the compound, deduced from the Tauc plot of the absorption spectrum, indicated a wide energy gap of 3.65 eV.

Keywords Flucytosine · Crystal structure · Cadmium compound · Hirshfeld surface analysis · IR · UV-visible

Introduction

The chemistry of drug salts and cocrystals is commonly employed to create a wide range of supramolecular architectures with potential applications [1–6]. Metal ion interactions with nucleobases have garnered a lot of attention in biological science over the last few decades [7–10]**.** Among these, cadmium(II) ion–nucleobase interactions are of current interest [11–13]. Although free Cd(II) ion is well known for its high toxicity to human health, several research studies have shown that Cd(II) compounds with organic ligands have interesting bio-activities such as DNA binding [14, 15], antitumor [16, 17], and antibacterial [18, 19]. Several drugs and their metal compounds, including cytosine and its analogs, have been tested for fungicidal and fungistatic activities [20, 21]. Flucytosine (also known as 5-fluorocytosine or 5FC) is an established antifungal agent with a long history of use [22]. Although it was first synthesized in 1957, its potent antifungal properties were not recognized until 1964 when it demonstrated activity against Cryptococcus neoformans and Candida species [23]. Although it lacks inherent antifungal properties, once absorbed by vulnerable fungal cells, it undergoes a transformation into 5-fluorouracil (5-FU). Subsequently, this compound is converted into metabolites that hinder the synthesis of fungal RNA and DNA [24]. Two recent developments have sparked renewed interest in 5FC: It is increasingly used in combination with azole antifungal agents such as ketoconazole, fluconazole, and itraconazole; and it plays a crucial role in a new therapeutic strategy in

✉ Hela Ferjani
hhferjani@imamu.edu.sa

1 Chemistry Department, College of Science, Imam Mohammad Ibn Saud Islamic University (IMSIU), 11623 Riyadh, Saudi Arabia

2 Department of Chemistry, King Fahd University of Petroleum and Minerals, 31261 Dhahran, Saudi Arabia

3 Interdisciplinary Research, Center for Refining and Advanced Chemicals, King Fahd University of Petroleum & Minerals, 31261 Dhahran, Saudi Arabia

4 Materials Science Innovation and Modelling (MaSIM) Research Focus Area, Faculty of Natural and Agricultural Science, North-West University (Mafikeng Campus), Private Bag X2046, Mmabatho 2735, South Africa

5 Department of Chemistry, Faculty of Natural and Agricultural, Science, North-West University (Mafikeng Campus), Private Bag X2046, Mmabatho 2735, South Africa

the treatment of certain cancerous cells, notably *colorectal carcinoma* [25]. It exerts its antifungal effects by interfering with both deoxyribonucleic acid (DNA) and protein synthesis [26].

In this current study, Cd(II) compound of 5-Flucytosine (5FC) was synthesized in order to study the structural interaction of the metal ion and the organic moiety, as well as the non-covalent interaction in the supramolecular assembly. A search in CSD version 5.41 (November 2019) reveals 56 structures based on flucytosine as polymorphs, hydrates, solvates, salts, and cocrystals. Thirty-three of them crystallized in the monoclinic crystalline system, in the $P2_1/c$, $P2_1/n$, $P2_1/m$, $P2_1/a$, C2/c and Cc space groups. Twenty-one crystallized in the triclinic $P\bar{1}$ space group, as well as a few others ($P4_12_12$, Pbca) [19, 27–36]. From these numbers, it is possible to observe that neutral state is most common for the 5-Flucytosine. Furthermore, studies on metal compounds and flucytosine salts have been limited and this has motivated the current study. The aim was to explore more structural understanding and offer conceptual illumination of this topic, since numerous components of this molecule's reactivity with metals have yet to be examined. However, a search of CSD for metal compounds of 5FC gives a single hit of a Zn(II) compound (refcode VEZQUP) having the formula, $[ZnBr_2(5FC)(H_2O)].(5FC)$. In this, the Zn(II) ion is tetracoordinated, and the 5FC ligand is attached to zinc in a monodentate fashion by the nitrogen atom of the pyrimidine ring. Metal complexes of (5FC) might theoretically include the coordination via the N or O atoms of the pyrimidine ring and the N atom of the amino substituent. To determine how these possibilities will be realized, we prepared a new cadmium compound with 5FC, $(H\text{-}5FC)_2[(5\text{-}HFC)_2Cd_3Cl_{10}]$, and report its coordination mode, hydrogen bond pattern, supramolecular architecture, Hirshfeld surface analysis, and optical absorption.

Experimental

Materials and physical measurements

All reagents and solvents were obtained commercially from Sigma-Aldrich and used without any further purification. The CHN analyses were performed on an Elementary, Vario EL Cube, set up for CHNS analysis. The absorption spectrum of the powdered (1) compound was measured at room temperature with a JASCO V-770 spectrophotometer in the wavelength range 200–700 nm, using BaSO4 plates as a reference. Infrared spectrum was recorded using Agilent Cary 630 Fourier transform infrared spectrophotometer (FTIR) in the 4000–400 cm^{-1} spectral region with a single clean crystal.

Synthesis of $(H\text{-}5FC)_2[(H\text{-}5FC)_2Cd_3Cl_{10}]$

A hot solution (8 mL) of flucytosine (0.258 g, 2 mmol) and 2 mL of concentrated HCl (Scheme 1) was added to a solution of $Cd\text{-}Cl_2.H_2O$ (0.201 g, 1 mmol) in 10 mL of distilled water and 2 mL of concentrated HCl. The pH of the solution was around 2. The reaction mixture was refluxed for 4 h before being reduced to approximately 10 mL. This product solution was kept unperturbed in a 50 ml beaker and colorless needle shaped crystals appeared after 30 days.

Yield of 72.7%, MPt, 156 °C. Analysis calculated (%) for $C_{16}H_{20}Cd_3Cl_{10}F_4N_{12}O_4$: C 15.85, H 1.66, N 13.87; found C 15.80, H 1.52, N 13.68.

Crystallography

A single crystal of $(H\text{-}5FC)_2[(H\text{-}5FC)_2Cd_3Cl_{10}]$ suitable for crystal structure analysis was obtained by slow evaporation of the mother liquor at room temperature. Data were collected at 298 K using the Bruker APEX3 software package on a Bruker AXS D8 Quest Diffractometer (MoKα radiation, $\lambda = 0.71073$ Å) [37]. Data reduction was performed using SAINT [38]. The structure was solved with the ShelXT [39] structure solution program and refined with the ShelXL [40] refinement package using least squares minimization on F^2. Data were corrected for absorption using the numerical method (SADABS) based on crystal dimensions [41]. All non-hydrogen atoms were refined with anisotropic displacement parameters, while all hydrogen atoms were placed at geometrical estimates and refined using the riding model. The illustrations were drawn by Ortep 3[42] and Mercury [43]. Selected interatomic distances and bond angles are presented in Table 1S in the Supporting. Details of crystal refinement and data collection for $(H\text{-}5FC)_2[(H\text{-}5FC)_2Cd_3Cl_{10}]$ are given in Table 1.

Results and discussion

Synthesis and physical properties

The reaction proceeds firstly by the protonation of the drug using HCl in order to improve its solubility in water and enhance the reactivity with the metal ion. The subsequent synthesis reaction at elevated temperature resulted in additional reaction via the oxygen atom of the drug. A slow evaporation of the colorless solution crystallized the product as needle shaped crystals after 30 days. The

Table 1 Crystallographic data and structure refinement parameters of (1)

Chemical formula	$(H\text{-}5FC)_2[(H\text{-}5FC)_2Cd_3Cl_{10}]$
CCDC number	2,249,554
M_r (g/mol)	1212.14
Crystal system, space group	Triclinic, $\bar{1}$
Temperature (K)	298
a/b/c (Å)	9.6805 (11) / 9.8121 (12) / 10.5720 (13)
$\alpha/\beta/\gamma$ (°)	67.019 (6) / 69.961 (6) /81.662 (6)
V (Å^3)	868.45 (19)
Z	1
μ (mm^{-1})	2.66
D_x (Mg m^{-3})	2.318
F(000)	582
Crystal size (mm)	0.21 × 0.15 × 0.05
$\theta_{min}/\theta_{max}$ (°)	2.2/28.3
No. of measured/independent/observed [I > 2σ(I)] reflections	86,345/4316/3880
R_{int}	0.151
Data/Restraint/parameters	4316/0/223
$R[F^2 > 2\sigma(F^2)]$	0.051
wR(F^2)	0.140
S = GOOF	1.19
$\Delta\rho_{max}/\Delta\rho_{min}$ (e.Å^{-3})	4.00/− 2.10

compound, $(H\text{-}5FC)_2[(H\text{-}5FC)_2Cd_3Cl_{10}]$, was found to be soluble in alcohols but insoluble in nonpolar solvents including chloroform, hexane, and dichloromethane.

Structure description

The compound (1) belongs to the triclinic crystal system and P $\bar{1}$ space group. The crystal structure consists of two unique Cd(II) ions Cd1 and Cd2 of which Cd2 is located in an inversion center. Additionally, there are five chloride anions, with Cl1 and Cl2 acting as terminal ligands, while the remaining chloride ions serve as bridging ligands. Furthermore, there are two crystallographically independent protonated 5FC cations. One of these cations coordinates with Cd1, while the other independent $(H\text{-}5FC)^+$ cation serves as a charge balancing species (Fig. 1). Bond lengths and angles of anionic and cationic moieties are listed in Tables 1S. The two cadmium atoms have an octahedral coordination environment. The central Cd2 is hexacoordinated by six chlorine atoms. The Cd1 atom is octahedrally surrounded by five Cl^- ions and one protonated $[H\text{-}5FC]^+$ ligand through the O1 atom. Such that the two distorted octahedral units are linked by sharing a common face, using three μ_2-bridging modes (μ_2-Cl3, μ_2-Cl4 and μ_2- Cl5). This gives rise to a zig-gag subunit with Cd1-Cd2-Cd1 angle of 180° that runs along *b*-axis (Fig. 1S, Table 1S).

The geometrical parameters of the octahedron, Cd-Cl distances (2.4942 (10) Å to 2.7382 (10) Å), d(Cd-O1) = 2.485 (3) Å and Cl–Cd–Cl bond angles (80.36 (3)°-180.0° are comparable to those of previously reported anions [44–46]. The Cd-μ_2-Cl is longer than the terminal Cd-$Cl_{1,2}$. The Cd1···Cd2 distance is 3.3536 (5) Å, which is greater than the sum of cadmium Van der Waals radii (3.2 Å), indicating that there are no effective intermetallic interactions between them. The protonated $[H\text{-}5FC]^+$ ligand is planar (r.m.s deviation = 0.0084 Å) and linked the octahedron by its oxygen atom with Cd–O distance of 2.485 (3) Å. The anionic moieties are balanced by

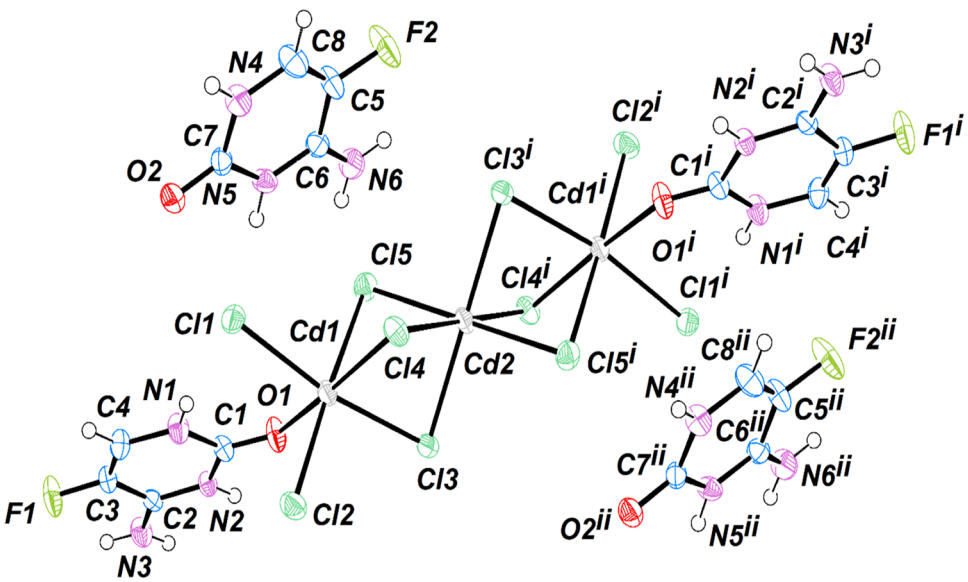

Fig. 1 The ORTEP diagram of the molecular structure of (1). The ellipsoids are drawn at the 50% probability level. (Symmetry codes: (i) − *x*, − *y*, − z; (ii) *x*, *y*− 1, *z* + 1)

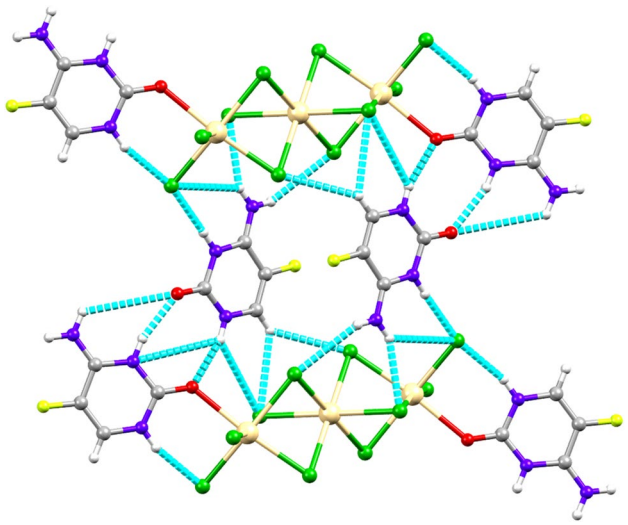

Fig. 2 Hydrogen bonding interactions in (1)

Table 2 Intermolecular hydrogen bonding parameters of (1)

D–H···*A*	H···A (Å)	D···A (Å)	D–H···A (°)
C8-H8···Cl4^{ii}	2.96	3.723 (4)	140
N6-H6B···Cl3^{i}	2.80	3.393 (4)	127
N6-H6B···Cl2^{iii}	2.72	3.463 (4)	145
N6-H6A···Cl5	2.58	3.354 (4)	150
N5-H5···Cl1	2.24	3.103 (3)	176
N4-H4···O1^{iv}	2.04	2.872 (4)	162
N3-H3B···Cl3^{v}	2.86	3.385 (3)	121
N3-H3B···Cl2^{vi}	2.70	3.494 (4)	154
N3-H3A···Cl2^{v}	2.48	3.239 (3)	148
N2-H2···O2^{vii}	1.98	2.813 (4)	163
N1-H1···Cl1	2.29	3.112 (3)	159
C8-H8···Cl4^{ii}	2.96	3.723 (4)	140
N6-H6B···Cl^{3i}	2.80	3.393 (4)	127
N6-H6B···Cl2^{iii}	2.72	3.463 (4)	145
N6-H6A···Cl5	2.58	3.354 (4)	150
N5-H5···Cl1	2.24	3.103 (3)	176
N4-H4···O1^{iv}	2.04	2.872 (4)	162
N3-H3B···Cl3^{v}	2.86	3.385 (3)	121
N3-H3B···Cl2^{vi}	2.70	3.494 (4)	154
N3-H3A···Cl2^{v}	2.48	3.239 (3)	148
N2-H2···O2^{vii}	1.98	2.813 (4)	163
N1-H1···Cl1	2.29	3.112 (3)	159

Symmetry codes: (i) $-x, -y, -z+2$; (ii) $-x, -y, -z+1$; (iii) $x-1, y, z$; (iv) $x, y, z-1$; (v) $-x+1, -y+1, -z+2$; (vi) $x, y+1, z$; (vii) $x, y, z+1$

independent $[H\text{-}5FC]^+$ cations that occupy the cavities on both sides of the inorganic chains in a zig-zag motif (Pink cations in Fig. 1S). These organic cations interact with the inorganic chains through N/C-H···Cl and N–H···O hydrogen bonds, contributing to a three-dimensional hydrogen bond network (Fig. 2, Table 2). From the supramolecular crystal structure of this compound, it can be seen that the stability of the compound is ensured by non-classical Y-X···π interactions that occurs between chlorine atoms Cl1 and Cg8 (Cd1-Cl1···Cg8), where Cg8 is the centroid of independent $[H\text{-}5FC]^+$ cation (Fig. 3a**,** Table 3) and between oxygen of independent cations O2 and Cg7 (C7-O2···Cg7), where Cg7 is the centroid of the chelating ligand. Furthermore, X···Y non-covalent interactions type F···F (2.668 Å) interactions between cation and anion moieties in the structure also assure the cohesion of the structure (Fig. 3b).

Infrared spectroscopy study

The vibrational spectra of the complex and the free ligand were analyzed (for comparison) and presented in Figs. 3S and 4S, respectively. The spectrum of the ligand shows peaks at 3340 and 3310 cm^{-1}, which are identified as the antisymmetric and symmetric N–H stretching vibrations, respectively. The spectrum also showed the C=O vibration at 1659 cm^{-1}, while the C–F stretching vibrations are observed in the 1100–1200 cm^{-1} region. In coordinated complexes, the functional groups of the ligands in the proximity of the ligating atoms slightly shift depending on the bonding fashion and the size of the metal ion. Figure 4S shows the characteristic band of a coordination compound with a protonated 5FC moiety. The asymmetric stretching mode due to the N–H of an aliphatic amine NH_2 group appears at 3322 cm^{-1}, which is higher than that of the symmetrical one (3056 cm^{-1}). The band at 3117 cm^{-1} is assigned to NH of pyrimidine ring. This peak often appears at a lower frequency region compared to the free ammine group. In the current study, it is about 200 cm^{-1} less, indicating a weakening of the vibrational frequency due to the proximity to the ligating O atom. The band observed at 2936 cm^{-1} is assigned to C–H stretching vibration, while those at 1661 and 1212 cm^{-1} are assigned to the stretching modes of C=C and C–C bonds, respectively. The C=N and C–N stretching vibrations appeared at 1693 and 1277 cm^{-1}, respectively. Silverstein et al. [47] assigned the stretching vibration of C–N in the region of 1342–1220 cm^{-1}. However, in the coordinated 5FC, this position is bound to change due to the metal–ligand bond. The vibrational peak at 1718 cm^{-1} can be attributed to the C=O stretching mode, while the C–F vibrational mode is located at 1196 cm^{-1}. The reported peaks conform with the peak assignments in previous studies [48–51].

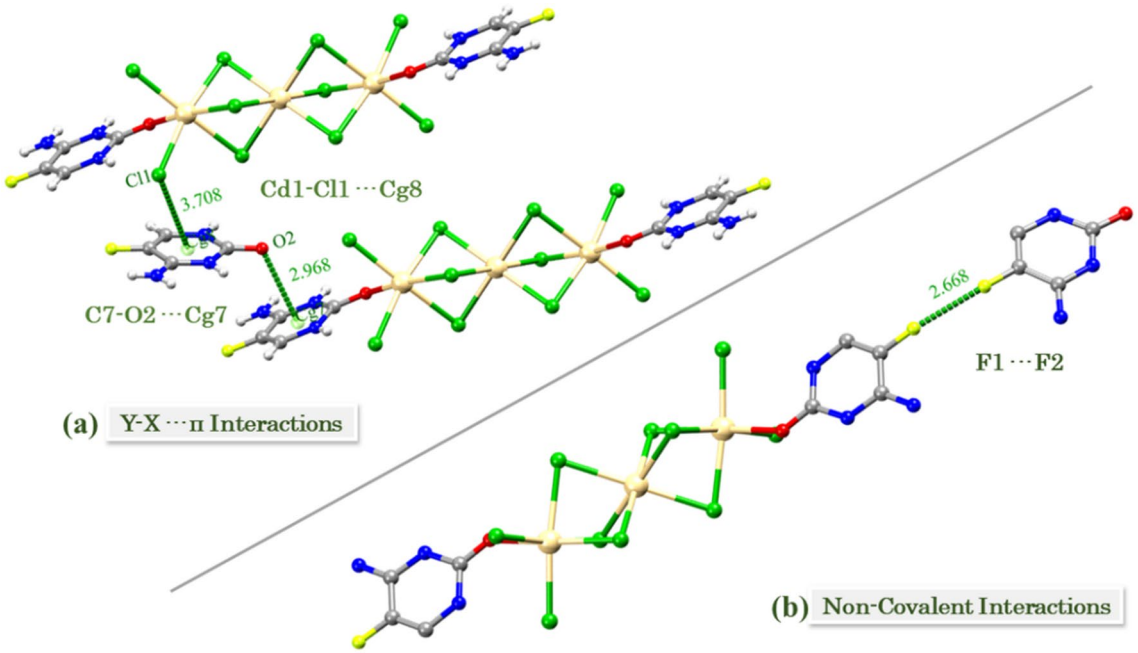

Fig. 3 A view of **a** *Y-X*···π interactions in (1) and **b** the anion–anion interaction

Table 3 Y-X···Cg interactions parameters for (1)

	Y···X (Å)	d(X···Cg) (Å)	d(Y···Cg) (Å)	Y-X···Cg(°)
Cd1-Cl1···Cg8^{viii-}	2.541 (1)	3.708(2)	5.009(2)	105.02(4)
C7-O2···Cg7^{viii}	1.224 (5)	2.968(4)	3.688(5)	117.0(3)

Symmetry codes: (viii) $x,1-y,1-z$; (viiii) $x,1-y,1-z$

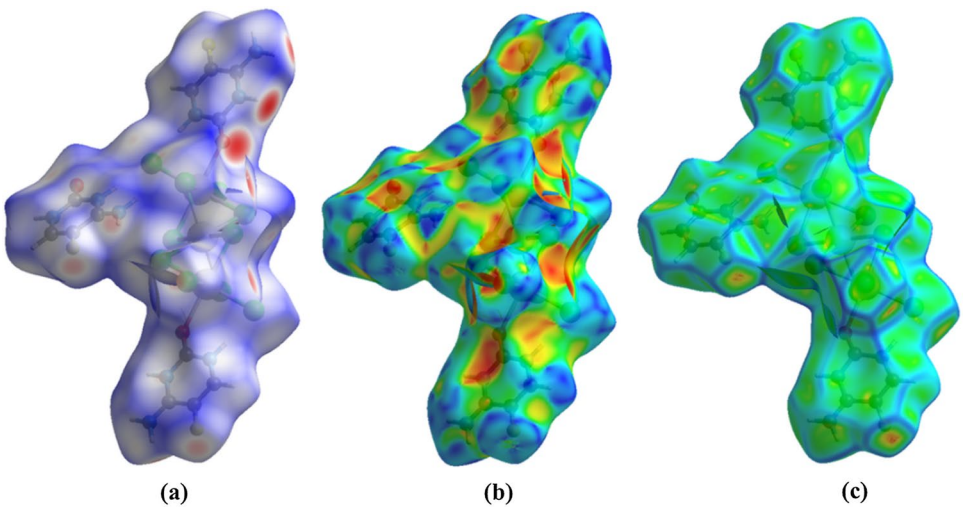

Fig. 4 **a** d_{norm} mapped on Hirshfeld surfaces for visualizing the intermolecular interactions, **b** shape index, and **c** curvedness of $(H\text{-}5FC)_2[(H\text{-}5FC)_2Cd_3Cl_{10}]$

Hirshfeld surface analysis

The Hirshfeld surface analysis (HS) [52] and the associated 2D fingerprint plots [53] were generated using CrystalExplorer17 program [54]. Figure 4 depicts the mapping of the Hirshfeld surface of (1) onto d_{norm} (a) ranging from − 0.597 to 1.109 Å, shape index (b) ranging from -0.998 to 0.998 Å, and curvedness (c) ranging from − 3.821 to 0.435 Å. The d_{norm} mapping shows a bright red region in the Hirshfeld surface, indicating that hydrogen bonding interactions are dominant in the structure. These interactions include N/C-H···Cl/O hydrogen bonding between chlorine atoms in

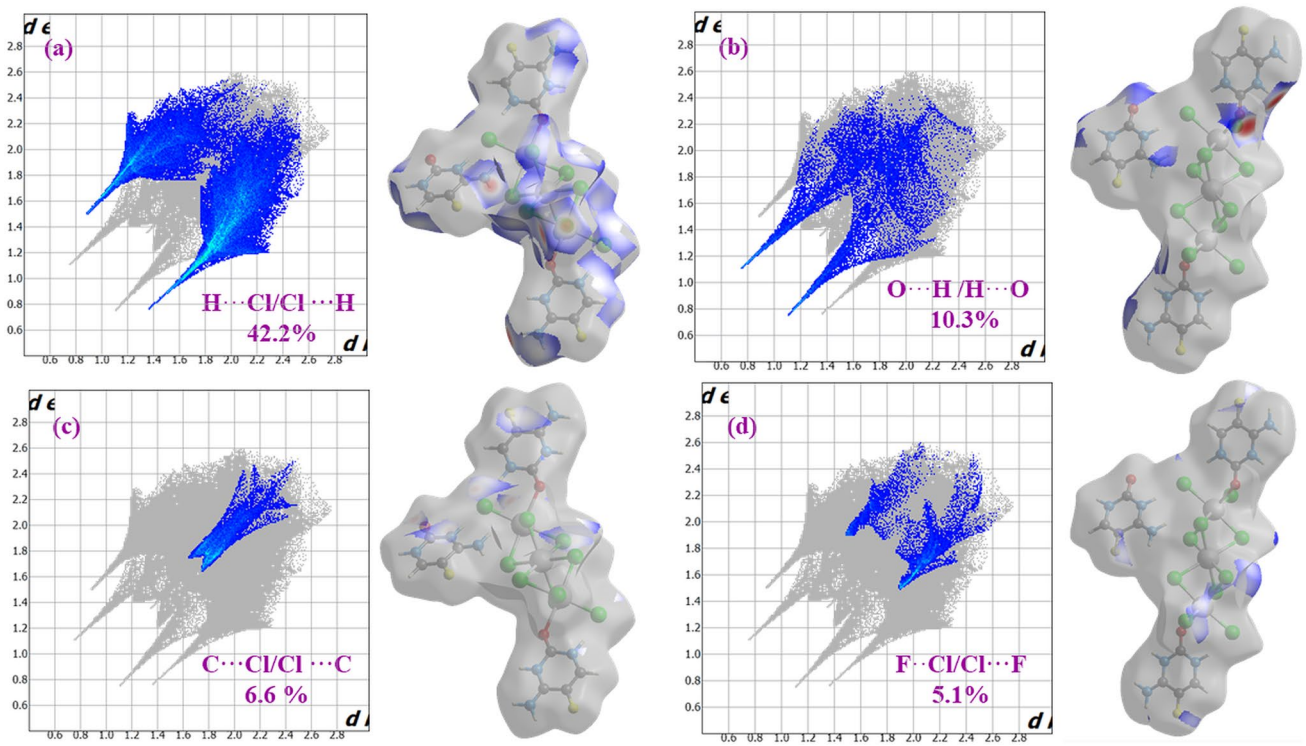

Fig. 5 Fingerprint plots with fragment patches of **a** H···Cl, **b** O···H, **c** C···Cl and **d** F···Cl contacts in (1)

$[(H\text{-}5FC)_2Cd_3Cl_{10}]^{2-}$ and $(H\text{-}5FC)^+$ cations (Table. 2). Figures 5b and c show how shape index and curvedness surfaces were utilized to demonstrate π-stacking interaction patterns. The existence of red and blue triangles in the same region of the shape index surface (Fig. 4b) suggests that the π-stacking is present in the structure. Blue and red triangles depict the convex and concave regions generated by the carbon atoms in the molecule on the surface. Curvedness mapping on the Hirshfeld surface (Fig. 4c) depicts flat green patches divided by blue edges which is another feature of the π-stacking.

The overall 2D fingerprint plots for dominant contacts are shown in Fig. 5, together with their relative contributions to the Hirshfeld surface. The 2D fingerprint plots show that the dominant intermolecular H···Cl, O···H, Cl···C, and F···Cl interactions contribute 42.2%, 10.3%, 6.6%, and 5.1%, respectively, to the overall crystal packing. The fingerprint plot of H···Cl contacts corresponding to N/C-H···Cl interactions, which represent the largest contribution to the Hirshfeld surfaces (42.2%), shows two highly concentrated distinct spikes with a minimum value of $d_e + d_i = 2.8$ Å (Fig. 5a). The O···H interactions, which refer to N–H···O interactions appear as the second largest region of the fingerprint plot (10.3%) and have two distinct spikes having almost the same $d_e + d_i = 2.2$ Å (Fig. 5b). The 2D fingerprint map shows the third and fourth most abundant C···Cl and F···Cl contacts as a narrow and wide zone in the center, accounting for 6.6% (Fig. 5c) and 5.5% (Fig. 5d) of the total Hirshfeld surface area. The HS analysis reveals the presence of other interactions with low contributions that are summarized as a pie chart and presented in Fig. 2S.

Optical study

The optical absorption spectra of compound (1) and the (5FC) drug, recorded in the wavelength range of 200 nm-700 nm, are shown in Fig. 5S. Both spectrums exhibit a broad absorption band, with the highest peaks of absorption centered at 268 nm. These broad peaks were attributed to π-π* transition within the pyrimidine ring of 5FC drug [55]**.** The band gap energy of the sample was estimated using Tauc's formula [56]**,** which is given as:

$$(\alpha h\nu)^{1/n} = A\,(h\nu - E_g) \tag{1}$$

where A is a constant, h and ν are the Planck's constants and the photon frequency, respectively. The value of n is dependent on the type of compound; hence, $n = 1/2$ for direct and $n = 2$ for indirect semiconductor. The plot of $[\alpha h\nu]^2$ vs $h\nu$ (Fig. 5S) shows that the compound has a wide band gap of 3.65 eV. The compound has great potential for use in UV-sensitive applications such as coatings and solar cell window layers.

Conclusion

In the present study, a new cadmium compound (1), involving flucytosine moiety as a ligand and counter ion was synthesized and analytically characterized by UV–Visible spectroscopy. This compound, which crystallized in the P-1 space group, is made up of one independent protonated $[H\text{-}5FC]^{+}$ cation and half trinuclear $[(H\text{-}5FC)_2Cd_3Cl_{10}]^{2-}$ anion. These entities are joined together via hydrogen bonds, Cd1-Cl1···π interactions, and F···F non-covalent interactions, resulting in a three-dimensional network. The Hirshfeld surface analysis of the crystal structure indicates that the most important contribution for crystal packing is from H···Cl (42.2%) and H···O (10.3%) interactions and confirms the presence of Cl···π and F···Cl non-covalent interactions between different entities. The optical absorption shows that the compound's band gap is 3.65 eV, and it could be employed in UV-sensitive coatings and solar cell window layers.

Supplementary Information The online version contains supplementary material available at https://doi.org/10.1007/s11243-023-00562-7.

Author contributions H.F. and D.C.DO. wrote the main manuscript text, M.F analyzed the structure by SCXRD and refined the structure, N.S. A and N.P. R prepared figures and data analysis. All authors reviewed the manuscript.

Funding The authors extend their appreciation to the Deputyship for Research & Innovation, Ministry of Education in Saudi Arabia for funding this research through the project number IFP-IMSIU-2023114. The authors also appreciate the Deanship of Scientific Research at Imam Mohammad Ibn Saud Islamic University (IMSIU) for supporting and supervising this project.

Declarations

Conflict of interest The authors declared that there is no conflict of interest.

References

1. Hulme AT, Tocher DA (2006) Cryst Growth Des 6:481–487
2. Tilborg A, Norberg B, Wouters J (2014) Eur J Med Chem 74:411–426
3. Mohana M, Thomas MP, McMillen CD, Butcher RJ (2023) Acta Crystallog Sect C 79:61–67
4. Surampudi AVSD, Ramakrishna S, Pallavi A, Balasubramanian S (2023) CrystEngComm 25:1220–1231
5. Nechipadappu SK, and Balasubramanian S (2023) Acta Crystallographica section b: structural science, Crystal Eng Mater 79
6. Firmino PP, Pedro HDO, da Silva CC, de Araujo-Neto JH and Ellena J (2023) J Molecul Struct 136075
7. Mohapatra B, Verma S (2017) Chem Commun 53:4748–4758
8. Lippert B, Müller J (2016) Inorg Chim Acta 100:1–2
9. Sander SA, Morrow JR (2016) Inorg Chim Acta 452:90–97
10. Bartova S, Alberti E, Sigel RK, Donghi D (2016) Inorg Chim Acta 452:104–110
11. Capllonch MC, García-Raso A, Terrón A, Apella MC, Espinosa E, Molins E (2001) J Inorg Biochem 85:173–178
12. Muthiah PT, Robert JJ, Raj SB, Bocelli G, Ollá R (2001) Acta Crystallogr Sect E: Struct Rep Online 57:m558–m560
13. Stanley N, Muthiah PT, Luger P, Weber M, Geib S (2005) Inorg Chem Commun 8:1056–1059
14. Waalkes MP, Poirier LA (1984) Toxicol Appl Pharmacol 75:539–546
15. Khandar AA, Azar ZM, Eskandani M, Hubschle CB, van Smaalen S, Shaabani B, Omidi Y (2019) Polyhedron 171:237–248
16. Luo H-Y, Li J-Y, Li Y, Zhang L, Li J-Y, Jia D-Z, Xu G-C (2016) RSC Adv 6:114997–115009
17. Fedorov B, Fadeev M, Utenyshev A, Shilov G, Konovalova N, Tatyanenko L, Sashenkova T, Blokhina S, Berseneva E (2011) Russian Chem Bull 60:1959–1962
18. Montazerozohori M, Zahedi S, Nasr-Esfahani M, Naghiha A (2014) J Ind Eng Chem 20:2463–2470
19. You ZL, Zhu HL (2006) Z Anorg Allg Chem 632:140–146
20. Netalkar PP, Netalkar SP, Revankar VK (2015) Polyhedron 100:215–222
21. Azam M, Khan AA, Al-Resayes SI, Islam MS, Saxena AK, Dwivedi S, Musarrat J, Trzesowska-Kruszynska A, Kruszynski R (2015) Spectrochim Acta Part A Mol Biomol Spectrosc 142:286–291
22. Grunberg E, Titsworth E, Bennett M (1964) Chemotherapeutic activity of 5-fluorocytosine 566–568
23. Vermes A, Guchelaar H-J, Dankert J (2000) J Antimicrob Chemotherapy 46:171–179
24. Benson J, Nahata M (1988) Clin Pharm 7:424–438
25. Nyati M, Symon Z, Kievit E, Dornfeld K, Rynkiewicz S, Ross B, Rehemtulla A, Lawrence T (2002) Gene Ther 9:844–849
26. Delma FZ, Al-Hatmi AM, Brüggemann RJ, Melchers WJ, de Hoog S, Verweij PE, Buil JB (2021) J Fungi 7:909
27. Portalone G, Colapietro M (2006) Acta Crystallogr Sect E Struct Rep Online 62:o1049–o1051
28. Tutughamiarso M, Bolte M, Egert E (2009) Acta Crystallogr C 65:o574–o578
29. Da Silva CC, de Oliveira R, Tenorio JC, Honorato SB, Ayala AP, Ellena J (2013) Cryst Growth Des 13:4315–4322
30. Prabakaran P, Murugesan S, Muthiah PT, Bocelli G, Righi L (2001) Acta Crystallogr Sect E Struct Rep Online 57:o933–o936
31. Portalone G, Colapietro M (2007) J Chem Crystallogr 37:141–145
32. Perumalla SR, Pedireddi VR, Sun CC (2013) Cryst Growth Des 13:429–432
33. Perumalla SR, Pedireddi VR, Sun CC (2013) Mol Pharm 10:2462–2466
34. Portalone G (2011) Chem Cent J 5:1–8
35. Tutughamiarso M, Wagner G, Egert E (2012) Acta Crystallogr B 68:431–443
36. Tutughamiarso M, Egert E (2012) Acta Crystallogr B 68:444–452
37. Bruker BAI (2016) APEX3 Crystallography Software Suite, Madison, vol 2016. WI, USA
38. Bruker A, Saint A (2008) Acta Crystallogr Sect A Fundam Crystallogr 64:112
39. Sheldrick G (2015) Acta Crystallogr A 71:3–8
40. Sheldrick G (2015) Acta Crystallogr C 71:3–8
41. Sadabs BAI (2017) Madison. Wisconsin, USA
42. Farrugia L (1997) J Appl Crystallogr 30:565
43. Macrae CF, Sovago I, Cottrell SJ, Galek PTA, McCabe P, Pidcock E, Platings M, Shields GP, Stevens JS, Towler M, Wood PA (2020) J Appl Crystallogr 53:226–235
44. Qin L-L, Ye H-Y, Wang D-Y (2014) Inorg Chem Commun 46:47–50
45. Sun X-F, Wang Z, Liao W-Q, Li P-F, Gao J, Huang Y-Y, Chen H-P, Ye H-Y, Zhang Y (2017) RSC Adv 7:52024–52029

46. Karthikeyan A, Zeller M, Thomas Muthiah P (2018) Acta Crystallogr Sect C Struct Chem 74:789–796
47. Silverstein RM, Bassler GC (1962) J Chem Educ 39:546
48. Palafox MA, Rastogi VK (2015) Asian Chem Lett 19:01–2533
49. Gunasekaran S, Seshadri S, Muthu S (2006) Indian J Pure Appl Phys 44:581–586
50. Sharma V, Sharma S, Sharma V (1995) Asian J Chem 7:855
51. Seshadri S, Gunasekaran S, Muthu S, Kumaresan S, Arunbalaji R (2007) J Raman Spectro Int J Orig Work Asp Raman Spectro Includ Higher Order Process Brillouin Rayleigh Scatter 38:1523–1531
52. Spackman MA, Jayatilaka D (2009) CrystEngComm 11:19–32
53. Spackman MA, McKinnon JJ (2002) CrystEngComm 4:378–392
54. Spackman PR, Turner MJ, McKinnon JJ, Wolff SK, Grimwood DJ, Jayatilaka D, Spackman MA (2021) J Appl Crystallogr 54:1006–1011
55. Cavalieri LF, Bendich A (1950) J Am Chem Soc 72:2587–2594
56. Makuła P, Pacia M, Macyk W (2018) ACS Publications, pp. 6814–6817

Terms and Conditions

Springer Nature journal content, brought to you courtesy of Springer Nature Customer Service Center GmbH (“Springer Nature”).
Springer Nature supports a reasonable amount of sharing of research papers by authors, subscribers and authorised users (“Users”), for small-scale personal, non-commercial use provided that all copyright, trade and service marks and other proprietary notices are maintained. By accessing, sharing, receiving or otherwise using the Springer Nature journal content you agree to these terms of use (“Terms”). For these purposes, Springer Nature considers academic use (by researchers and students) to be non-commercial.
These Terms are supplementary and will apply in addition to any applicable website terms and conditions, a relevant site licence or a personal subscription. These Terms will prevail over any conflict or ambiguity with regards to the relevant terms, a site licence or a personal subscription (to the extent of the conflict or ambiguity only). For Creative Commons-licensed articles, the terms of the Creative Commons license used will apply.
We collect and use personal data to provide access to the Springer Nature journal content. We may also use these personal data internally within ResearchGate and Springer Nature and as agreed share it, in an anonymised way, for purposes of tracking, analysis and reporting. We will not otherwise disclose your personal data outside the ResearchGate or the Springer Nature group of companies unless we have your permission as detailed in the Privacy Policy.
While Users may use the Springer Nature journal content for small scale, personal non-commercial use, it is important to note that Users may not:

1. use such content for the purpose of providing other users with access on a regular or large scale basis or as a means to circumvent access control;
2. use such content where to do so would be considered a criminal or statutory offence in any jurisdiction, or gives rise to civil liability, or is otherwise unlawful;
3. falsely or misleadingly imply or suggest endorsement, approval , sponsorship, or association unless explicitly agreed to by Springer Nature in writing;
4. use bots or other automated methods to access the content or redirect messages
5. override any security feature or exclusionary protocol; or
6. share the content in order to create substitute for Springer Nature products or services or a systematic database of Springer Nature journal content.

In line with the restriction against commercial use, Springer Nature does not permit the creation of a product or service that creates revenue, royalties, rent or income from our content or its inclusion as part of a paid for service or for other commercial gain. Springer Nature journal content cannot be used for inter-library loans and librarians may not upload Springer Nature journal content on a large scale into their, or any other, institutional repository.
These terms of use are reviewed regularly and may be amended at any time. Springer Nature is not obligated to publish any information or content on this website and may remove it or features or functionality at our sole discretion, at any time with or without notice. Springer Nature may revoke this licence to you at any time and remove access to any copies of the Springer Nature journal content which have been saved.
To the fullest extent permitted by law, Springer Nature makes no warranties, representations or guarantees to Users, either express or implied with respect to the Springer nature journal content and all parties disclaim and waive any implied warranties or warranties imposed by law, including merchantability or fitness for any particular purpose.
Please note that these rights do not automatically extend to content, data or other material published by Springer Nature that may be licensed from third parties.
If you would like to use or distribute our Springer Nature journal content to a wider audience or on a regular basis or in any other manner not expressly permitted by these Terms, please contact Springer Nature at

onlineservice@springernature.com